Best Practice

Analyzing Urban Land Cover and Demographic Shifts through Remote Sensing Technologies

Swarup Nugehalli[1,*], Peder Nelson[2], and Russanne Low[3]

[1] 11th Grade, Lawrence D. Bell High School; https://orcid.org/0009-0007-0157-4646.
[2] Oregon State University; peder.nelson@oregonstate.edu; https://orcid.org/0000-0003-3979-9051.
[3] Institute for Global Environmental Strategies; low.russanne@gmail.com; https://orcid.org/0000-0002-7912-4350
[*] Corresponding Author: swarupnugehalli@gmail.com; (+1) 817-368-1434

Abstract: This study investigates patterns of urban land cover change in Euless, Texas, using an integrated framework of satellite remote sensing and field-based observation. A 900-hectare area of interest was divided into a 37-point sampling grid, where ground photographs were collected using the GLOBE Observer application to validate and interpret satellite-derived classifications. Multiple remote sensing datasets, including Landsat Time Series Explorer (normalized burn ratio, NBR), ESRI Land Cover (2017/2024), WorldCover 10 m, Dynamic World (2016/2024), Meta/WRI Global Canopy Height, and MRLC NLCD Fractional Impervious Surfaces, were analyzed to quantify changes in built-up area, vegetation cover, canopy height, and surface imperviousness over time. Results indicate a clear increase in built-up land and impervious surfaces across much of the study area, accompanied by an overall reduction in tree canopy; however, localized anomalies in the southwestern portion of the area of interest, especially at sampling points 25 and 26 of the area of interest, demonstrated sustained canopy density and improved vegetation health, with exemplified NBR values increasing over the years. These findings highlight the spatial heterogeneity of urban growth and demonstrate that remote sensing, when validated with field observations, can effectively identify both broad development trends and localized ecological stability within a suburban landscape.

Keywords: Landsat, Euless, remote sensing, urbanization, land cover

JOURNAL OF EARTH OBSERVATION & GEOSPATIAL APPLICATIONS

Academic Editor: Jeong Chang Seong
Received: 28 February 2026
Revised: 13 April 2026
Accepted: 20 April 2026
Published: 30 April 2026

1. Introduction

The transition from rural to urban environments has been a consistent global trend since the Industrial Revolution. Urbanization and population growth have dramatically reshaped landscapes around the world as a result of this demographic and geographic trend. As cities expand, natural ecosystems are either displaced or completely replaced by residential, commercial, and industrial zones, altering both environmental and social dynamics within the community and local area. The need for tracking, recording, and observing such effects on society followed a similarly dramatic rise as well. This necessity was met with the aid and support of remote sensing technologies, which have allowed changes on Earth's surface to be observed from space over time.

Remote sensing data collection methods can appear slightly ambiguous at first glance; however, most of it is rooted in simplicity when broken down to its fundamental components. Satellite imagery is a fundamental component of remote sensing, providing the primary data source for analyzing Earth's surface characteristics. The process involves a satellite or some sort of remote-sensing-based aircraft detecting changes in the physical characteristics of the land by recording the radiation which is emitted from the land (Kshetri, 2023). This is then interpreted through a scientific database, which produces comprehensive results and findings about the land cover in a certain area. These satellites or typically drone-based aircraft geo-reference, or map, the level of individual objects or even entire landscapes. At smaller geographic scales, higher amounts of land density and varying landscape features are allowed to be interpreted in similar ways (Singh, 2000). There are many ways remote sensing can be useful and utilized in a way that makes the most appropriate sense. For instance, some satellites or drones may record tree height or, in a slightly different way, the number of trees in a given area. These technologies could map the crown density of trees in a given plot of land or the density

Citation: Nugehalli, S., Nelson, P. & Low, R. (2026). Analyzing Urban Land Cover and Demographic Shifts Through Remote Sensing Technologies. Journal of Earth Observation and Geospatial Applications, 2(1), 39–50. https://doi.org/10.65372/zesm3j31

of the tree count in that same plot. The remote sensing data that can be extracted from such satellite imagery is instrumental in grasping a quantitative sense of how the land has changed with certain aspects and to what degree. Not only is remote sensing useful for the residential and commercial aspects of society, but it is also revered in chemical, biological, and military contexts. The satellites that work on the latter contexts tend to provide scientists with the same quality of data for remote areas in less developed countries as they do for urbanized areas in highly developed countries, such as New York City, NY, U.S.A. (Kshetri, 2023). The data that is provided through these satellites is not biased or favored in one area over another due to the holistic, uniform coverage that the technology offers. This style of obtaining data in a broader sense allows for the complex tasks to be broken down into smaller, simpler tasks that can be managed efficiently; for example, the census data of any larger population, such as the United States, tends to face issues with misrepresentation by overcounting or undercounting their demographics. The surveying methods that are being utilized to fix this issue involve the utilization of remote sensing satellites with greater accuracy and precision, especially since many remote sensing satellites orbit the earth at the same time every day and take pictures detailing how the land has changed. Overall, the general use of remote sensing allows for a great deal of development to occur properly, given the context of the land and how it has changed over a period of time.

Remote sensing data collection methods come in different forms as they aim to achieve slightly different goals. There are 2 main types of techniques in which remote sensing is utilized: active and passive sensing (Jia et al., 2021). Passive remote sensing, which tends to be the more traditionalized method for remote sensing in vegetation contexts, is analogous to a camera whose source of optical EM energy is the sun. When using passive remote sensing technology, natural energy such as solar energy sites is transmitted through, absorbed, emitted from, or reflected off an object or surface nearby, which is sensed by the satellite (Weishampel et al., 1996). The information that it reads from the reflections is then sent back in a visual way, which shows how the land has changed from previous pictures or media. This process is done by satellites such as the Landsat and NASA's Terra and Aqua remote sensing orbital technologies. There are, however, drawbacks with this method as only a fraction or small portion of the energy that is reflected from the surfaces encompasses the received signal. The magnitude of what is captured is highly dependent on the natural elements from the surrounding environment, which can consequently deem this traditional method of remote sensing inefficient, or at the very least, unreliable at times.

The other method of gathering data regarding land cover change involves active remote sensing. Active remote sensing functions similarly to a camera with a flash, since both the energy source and the sensor are located on the same medium. Since these active systems rely on their own source of illumination, they don't require nor are they reliant on sunlight or any solar angle to obtain important data regarding the land cover. Among these non-traditional active systems, radio detection and ranging is the most widely used, especially in forms such as synthetic aperture radar (SAR), which is commonly applied to forest canopy analysis (Waring et al., 1995). By functioning similarly to optical sensors, radar systems respond to the wavelength and spatial resolution of the instrument, but differ in what they exactly detect. Optical data is influenced primarily by pigment and moisture content, whereas radar signals, with wavelengths measured in centimeters, tend to respond to the structural and foundational characteristics of vegetation. Shorter radar wavelengths primarily interact with smaller canopy elements like leaves and twigs, while longer wavelengths penetrate deeper, which causes larger components such as branches or trunks to be more sensitive to the detection technology (Jia et al., 2021). Examples of active remote sensing satellites include Radarsat, NASA's ICESat-2, NASA's GPM core observatory, and Envisat. In this study, "demographic shift" is used in a descriptive sense to refer to observable changes in neighborhood composition and residential continuity reported in census-level summaries, rather than a directly modeled variable.

2. Study Area and Methods

2.1. Study Area

The area of interest (AOI) utilized for the studied area is Euless, Texas, which resides within the larger Hurst-Euless-Bedford mid-cities settlement, commonly referred to as HEB. This area is located in the larger Tarrant County in the north-central portion of the state and forms part of the broader Dallas-Fort Worth Metroplex. Euless lies just west of the Dallas/Fort Worth International Airport, and covers about 16.3 mi^2 (42.1 km^2). The city was officially incorporated in 1953, and over the decades, it has evolved from a smaller farming community into a suburban municipality with a diverse population and housing landscape, especially in the past fifteen years. Topographically, Euless is characterized by relatively flat terrain typical of the North Texas region, with gentle slopes, urban infrastructure, residential areas, commercial zones, and smaller remnants of older agricultural or semi-rural land uses in some areas as well. Its proximity to major transportation infrastructure, such as major highways (State Highways 183, 360, 820) and the DFW airport, has exacerbated its acceleration in suburbanization, making it a zone of both commuter residence and local economic activity. The built environment includes single-family homes, multi-family dwellings, retail zones, and many warehousing centers linked back to the airport, as mentioned earlier. In a demographic sense, Euless is notable for its diversity and recent immigrant community growth, with the significant influx of Nepalese and Tongan minority groups. As of 2023, 19.3% of residents were born outside the United States, and the median property value was $294,500, which highlights a middle-income suburban profile (Data USA, 2023). The city is about 47.8% White, 17.3% Black or African American, 13.4% Asian, 1.67% Native Hawaiian or Pacific Islander (US Census Bureau, 2024). In particular, however, the Tongan and broader Polynesian community has an immensely strong presence in and around Euless. The area is attractive due to its proximity to the airport and the employment opportunities that have arisen in recent years (Niche, n.d.). In addition to the established Tongan community, the Nepalese population exhibits a similar growth pattern within Euless. The city presents itself as a transitional suburban zone from pressures by urban development, transportation corridors, and housing sprawl, in contrast to the existing vegetation and open spaces from earlier decades. Euless combines a well-defined geographic footprint with active demographic and built-environment change. Its evolving community composition adds a social aspect to land-cover change that is often overlooked in conventional physical analyses. Consequently, Euless serves as a case study linking remote-sensing land cover data with demographic and community change, providing insight into the environmental and urban dynamics as well as the socio-spatial context of suburban transformation.

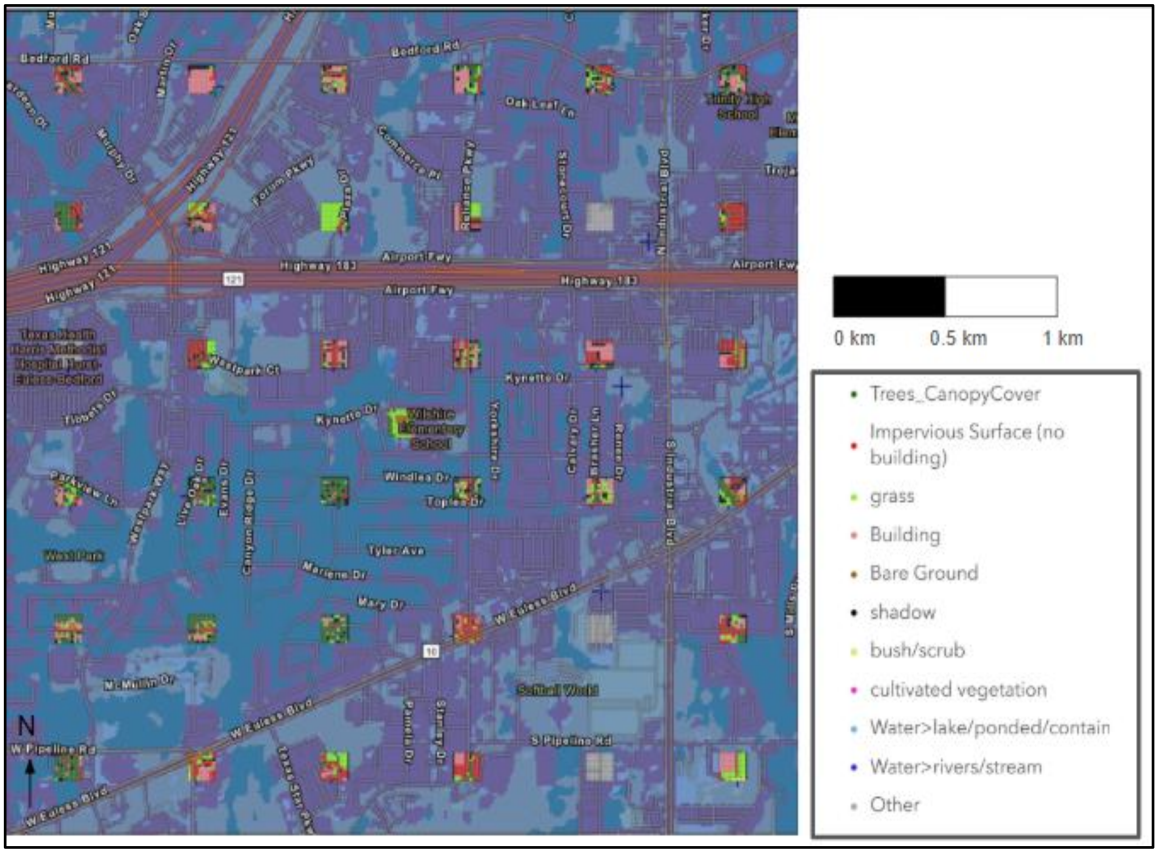

Figure 1. The area of interest surrounding the cities of the Hurst–Euless–Bedford region with land cover classifications derived from Collect Earth Online. Each color represents a classification (e.g., red = impervious surfaces, dark green = forest/trees). The grid represents a 3 km × 3 km (900 ha) study area. The map is oriented with north at the bottom left, and a scale bar is included to provide spatial reference.

2.2. Data

Euless proved to be agreeable in the context of land cover change and data within the ESRI 2017/2024, Collect Earth Online classifications, and Meta/WRI Global Canopy Height datasets. In this context, "agreeable" refers to datasets whose spatial resolution, temporal coverage, and classification schemes align well with the 3 km × 3 km (900 ha) AOI and the 37-point sampling grid, allowing for consistent comparison across models. Datasets that are not fully agreeable typically introduce inconsistencies due to mismatched spatial resolution, differing land cover definitions, or temporal gaps that may obscure short-term changes, particularly in heterogeneous suburban environments such as Euless where built and vegetated land are interwoven at fine scales. As a result, datasets with moderate-to-high spatial resolution and clearly defined classification structures were prioritized to improve comparability and reduce classification uncertainty across platforms.

The spatial and temporal resolutions of the datasets used in this study vary and directly influence their interpretability. The WorldCover dataset provides land cover classifications at a spatial resolution of approximately 10 m for 2020–2021, while the Dynamic World dataset also operates at approximately 10 m resolution with near-daily temporal updates spanning 2016–2024. The ESRI Land Cover dataset provides annual global classifications at approximately 10 m resolution for 2017 and 2024. In contrast, Landsat-based datasets, including the Landsat Time Series Explorer, operate at a coarser 30 m spatial resolution but offer a long-term temporal record from 1985 to 2025, making them well suited for identifying multi-decadal trends rather than fine-scale spatial variation. Similarly, the Meta/WRI Global Canopy Height dataset provides canopy height estimates at approximately 30 m resolution for circa 2020. These differences in resolution are important because higher-resolution datasets capture localized heterogeneity in suburban landscapes, while coarser-resolution datasets provide greater temporal continuity but may generalize smaller land cover features.

The ESRI dataset, when applied to the GeoJSON file of the AOI consisting of 37 different points (equally spaced from one another in a grid-like pattern), highlighted a growth of "Built Area" within the 900 ha area. The built area in 2017 was categorized as 881.3 ha, while "Trees" were categorized as 1.3 ha out of the entire area. The trend of increased urbanization and commercial development in commercial sectors presented itself as the Built Area grew to 892.1 ha in 2024, while Trees followed an expected inverse relationship, decreasing in coverage to about 0.4 ha. The Meta/WRI Global Canopy Height dataset shows that the average height of the tree canopy within the 900 ha sample area in 2020 is 5.47 meters, with a maximum canopy height of 23 meters and a minimum of 1 meter, likely representing shrubs or very young trees. Variability in canopy height is commonly influenced by multiple interacting ecological and anthropogenic factors, including forest age structure, urban management practices, and development-driven vegetation removal or pruning (Waring et al., 1995). As a result, canopy height differences can reasonably be interpreted as a combined signal of both natural growth conditions and human land-use intensity. These datasets were complementary to the data that the Dynamic World dataset produced when applied to the AOI. The Dynamic World 2016/2024 dataset showed that from 2016 to 2024, there was a significant change in Built Area, as it increased substantially from 813.67 ha in 2016 to 850.57 ha in 2024. This suggests a notable expansion of built-up areas in the analyzed region during those nine years, indicating continued urban development and sprawl.

The Landsat Time Series Explorer graphs for vegetated points utilized the normalized burn ratio (NBR), calculated using near-infrared (NIR) and shortwave infrared (SWIR) reflectance values derived from Landsat imagery, providing a spectral index for analysis. NBR is commonly used to assess vegetation health, biomass, and disturbance over time, making it appropriate for this study because it provides a long-term, consistent measure of vegetation condition that can be compared across decades of urban development. The graphs showed a logarithmic proportionality with NBR over 40 years from 1985 to 2025. For instance, the NBR was at 0.378 on July 31, 1989, whereas it was found to be 0.474 on July 31, 2006, indicating an increase in vegetation health that gradually stabilizes over time. The findings from the Landsat Time Series Explorer differ slightly from the other datasets, as they do not indicate a strong net decline in vegetation but instead show reduced growth rates or stabilization rather than consistent loss.

$$NBR = \frac{(NIR - SWIR)}{(NIR + SWIR)} \tag{1}$$

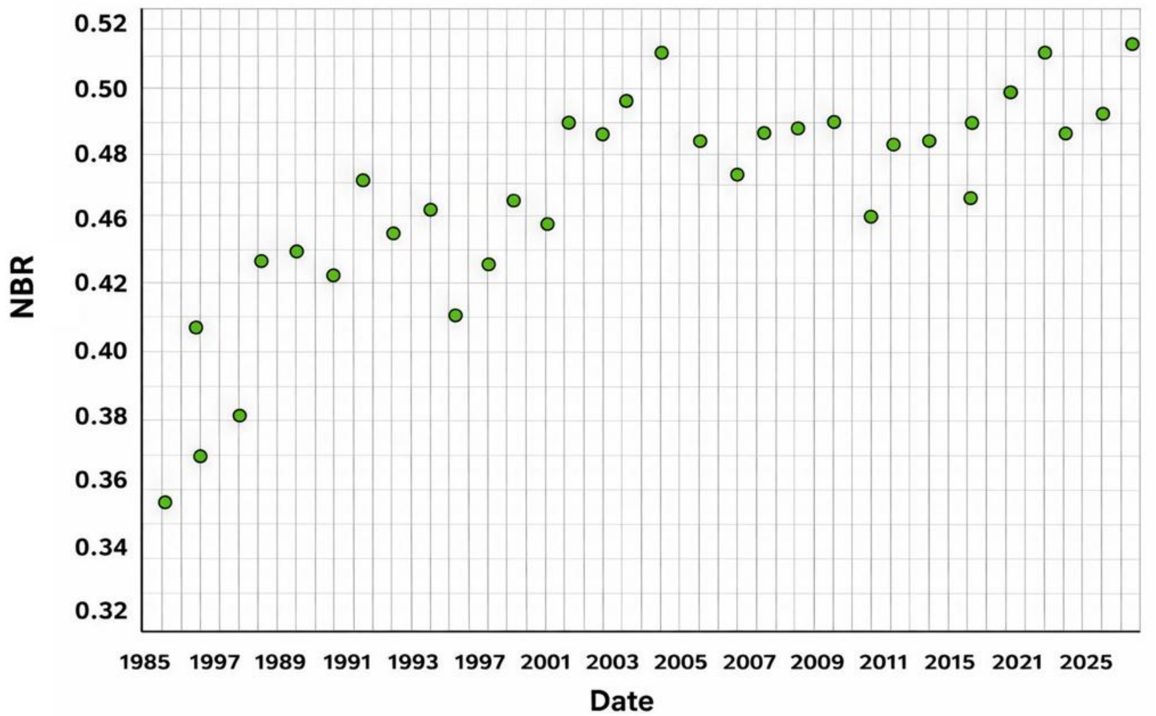

Figure 2. Landsat Time Series Explorer graph showing NBR trend of growth shown on point 26 of 37 in the AOI of Euless, TX. Point 26 is chosen to be an example as it falls under the area where there is comparable vegetation and tree growth. Courtesy of Google Earth Engine.

2.3. Methods

Many software and applications were utilized to obtain a thorough analysis of the AOI of Euless, Texas. One of these applications includes Global Learning and Observations to Benefit the Environment (GLOBE) Observer, a NASA-backed software that aids in the categorization of satellite data through field data, such as pictures. GLOBE Observer was the first field-based software to be used to gather the foundational fieldwork necessary for further analysis through other media (Kohl, 2019). The first step to examine such data was to take ground observations through the app.

Using the NESEC (NASA Earth System Explorers Community) geospatial sampling framework developed during the NASA SEES (STEM Enhancement in Earth Science) internship, an Area of Interest (AOI) was initially established consisting of 37 individual sampling units spanning approximately 900 ha. The centroid of the AOI was chosen accordingly, and a grid with 36 equidistant points was generated. The area of interest was inclusive of a 100 m^2 square-like grid, where point 0 was marked as the centroid of the square. Point 1 was marked as the most northwestern point, or in the top-most left miniature square. Points 2 through 6 followed a left-to-right pattern, with Point 7 returning to the left-most square in the row below. This pattern continued until Point 36, being the bottom-most right box. Once the grid was generated via Nesec, it was saved as both a CSV and a GeoJSON file, where all the information regarding the locations of each point was stored.

The GeoJSON file was uploaded to Google Maps to obtain traveling directions to the exact coordinates as generated by the SEES software. A few of the points were unable to be reached as they were closed off for various reasons, such as private vehicle lots or construction. In that case, the photos would not be included in the field observations as they would be highly inaccurate and undermine the integrity of the land cover analysis. Many of the points were placed in locations of private property or in front of residential areas, which made it harder to get permission for fieldwork observations; however, all of the points that were not blocked off, such as the aforementioned lots or construction areas, were able to be recorded and observed.

At the locations of each point, GLOBE Observer was used to take 6 photos in all cardinal directions, as well as photos marking an up and down direction for increased accuracy of the surrounding environment. Additional photos for distinction were able to be taken if deemed fit. Once the minimum of 222 photos were taken, they were uploaded to the NASA SEES 2025 server and approved for inspection. The pictures of each of the 37 different locations were able to be seen through the GLOBE Observer app after they were approved.

The AOI grid structure and spatial layout are presented in Figure 1, which illustrates the 3 km × 3 km study area and the distribution of the 37 sampling points used for analysis. At this stage, the necessary groundwork was complete, so many other applications, such as EarthMap, Collect Earth Online, and Landsat Time Series Explorer, were used to gather data about the land cover change over many years and the land cover itself at the time of observation.

Once the GeoJSON file was uploaded to EarthMap, a plethora of datasets were uncovered and were able to be layered to discern notable features regarding the land cover of not only each individual 100 m^2 box, which included each individual point as its center, but also the entire 900 ha area of interest as well. The datasets that were most useful and were included in observational examination included Land Cover - Dynamic World, ESRI 2017/2024, Meta/WRI Global Canopy Height, and WorldCover 10m 2020/2021 (ESA).

The Dynamic World dataset helped classify and uncover the Built Area, Trees, Grass, Shrub & Scrub, Bare Ground, Crops, and Water of the selected areas from the years 2016 and 2024, specifically. This was indicative of how the land had been utilized over a period of 8 years and provided a more precise characterization of what other factors were at play for the change to occur in such a specific manner. The ESRI layer showed how the combination of vegetation and the built environment relates to each other in the context of land cover. ESRI 2017/2024 showed a similar spread of classifiable characteristics such as Water, Trees, Flooded Vegetation, Crops, Built area, Bare Ground, Snow/Ice, Rangeland, and Clouds. The ESRI feature showed, in a similar fashion to the Dynamic World dataset, that the Trees and Built Area followed an inverse relationship with each other. The ESRI was able to include information regarding the reduction in both the rangeland and bare ground of the 900 ha area, which confirmed the classifications of the other datasets as well as the ground photos that were taken.

The Meta/WRI Global Canopy Height layer honed in on a specific type of land cover change in the area, which was highly useful in discovering potential causes for why the area is the way it is, not only in an environmental sense, but also in a demographic and social context. This layer showed the differing heights of tree canopy in the AOI grid on a scale from 2.00 meters to 30.00 meters, as well as how sparsely or densely populated some pockets of the AOI were with tree vegetation. This dataset helped highlight forest loss or gain over time and the social effects of that, such as whether or not deforestation or restoration efforts were made.

The WorldCover 10m 2020/2021 dataset included a more diverse crop-based spread of sub-categories to help increase the accuracy of what type of vegetation was present in the land, as opposed to classifying all vegetation as one section. The dataset included various factors such as Trees, Shrubland, Grassland, Cropland, Built-Up (urban development), Barren/Sparse Vegetation, Snow and Ice, Open Water, Herbaceous Wetland, Mangroves, and Moss and Lichen. In the Euless-based AOI, there were not many areas that could be classified under most of the subsections of vegetation, as the area is severely urban with pockets of trees, grassland, and cropland, mainly.

Collect Earth Online, or CEO, was used for investigation on the land cover which could not be classified through the other methods or datasets due to other factors such as vegetation or man-made structures blocking the observable land. CEO was used to manually record, declassify, and categorize the land of each of the 37 points to a far greater precision. Once the CSV file of the computer-generated grid was connected to the CEO server for the NASA SEES Earth System Explorer 2025 group, each location that was observed in the field showed up virtually on the CEO server with the help of aerial photographs.

Each picture, representing one point out of the 37 total points in the entire grid, was broken down into 100 equidistant points with different categories such as Tree Canopy Cover, Bush/Scrub, Cultivated Vegetation, Water (lakes and ponds), Water (rivers and streams), Water (irrigation), Shadows, Unknown, Bare Ground, Wet Land, and Impervious Surface. The goal of CEO was to compare the GLOBE Observer photos that were taken at the site with the aerial photos included in CEO's database for the specific point. An important part of the tedious process to note is that if the ground had a shadow due to tree canopy, it should be categorized as the land cover that was observed in the field, versus selecting shadow and moving on to the next point out of the 100.

This aimed to reduce the amount of unknown information regarding the environment. Since there were 100 smaller points to manually categorize, there were, consequently, 3,700 different points to categorize, which required lots of time to get through. Once each photo was complete with the manual categorizations, a confidence score from 0-100 was required for the observation, along with any notes that were helpful in the process of uncovering the conspicuous nature of the elements.

The Landsat time-series Explorer (LTSE) was used for quantitative reasoning and analysis, as it showed the growth of the healthy vegetation in a specific area once the coordinates of the latitude and longitude were inputted into Google Earth Engine. The NBR is a spectral index calculated from Landsat bands that's usually used to detect burn severity, vegetational health, and changes in biomass. The LTSE provides graphs of the NBR against the years from 1985 until 2025. A plateauing or stabilization in the NBR over time indicates that the area reached a stable vegetation cover due to likely urban landscaping or mature tree growth, whereas a constant increase in NBR would indicate a positive growth in healthy vegetation in the area, while the opposite holds true for a constant decrease over time. High values of NBR indicate high levels of healthy vegetation, whereas low values highlight low levels of healthy vegetation. Pictures of the given area were provided for each year as well to visually showcase the observable change that the land went through. The graphs of the NBR over time were provided and generated via Google Earth Engine Apps for every single point out of the 37 total grid markings.

The Multi-Resolution Land Characteristics (MRLC) National Land Cover Database (NLCD) was utilized to obtain individual data for each pixel in every image chip. The MRLC gave the data provided by the NLCD for each year for each chip from 1984 to 2024, allowing for extensive, thorough data to be analyzed. However, a limitation with this program was that it lacked precision, as there was a limit to how many decimal places could be inputted in each coordinate box. The miniature square box that encapsulated the specific point contained gradients of data on a scale from 0 to 100% for various datasets, such as tree canopy and impervious surfacing, among many more. This was done by downloading the NLCD for the datasets and combining them with the MRLC software. This analysis allowed for a thorough understanding of urban development as it visually tracked the change in different datasets for the many pixels of each individual image chip.

Due to the improving rates of urbanization in Euless, the dataset that seemed most appropriate to track was the FIS, or Fractional Impervious Surfaces. This sub-category allowed for the presentation of data in the aforementioned gradient style, which helped show how deeply affected a certain sub-region of the 100 m^2 box was by increased urbanization over the span of 40 years. The data derived from the FIS dataset is especially valuable because it provides a direct quantitative representation of how much of the land's surface has transitioned from natural or semi-permeable states (like grass or soil) to impervious ones, such as roads, buildings, and parking lots.

This information can then be correlated with environmental and socio-economic trends in the Euless area, such as population growth, infrastructure expansion, and rising housing density. A consistent increase in impervious surfaces indicates a higher degree of development and reduced capacity for water infiltration, which can have notable environmental consequences. These include increased surface runoff, higher flood risk, and elevated local temperatures due to the urban heat island effect. Over time, this expansion of impervious cover also leads to the fragmentation of natural habitats, limiting biodiversity and reducing the presence of tree canopy cover that plays an essential role in maintaining air quality and providing shade in urban areas. Ultimately, the use of the MRLC NLCD datasets, especially through the FIS sub-category, provided a dynamic visualization of Euless' transformation over four decades. It enabled a precise and accessible method of tracking patterns of growth, surface alteration, and the resulting environmental effects, which formed a foundational component of the study's analysis.

At the end of the study, ArcGIS was used to connect to the NASA SEES Earth System Explorers server, where a storyboard showing how the land cover change impacted different aspects of the area of interest was meant to be created. In the form of a website, the storyboard, or Community Chronicles, blended together both the foundational components on what made the AOI, or Euless in this case, what it was, as well as the present and future on how the land has and will change for either the better or worse and what impacts and repercussions that would have on social aspects of the community. To move beyond qualitative comparison between ground observations and satellite-derived classifications, a structured validation approach was applied using the GLOBE Observer field photographs as reference data.

Each sampled point was assigned a dominant land cover class based on field interpretation, which was then compared against the corresponding classification outputs from ESRI Land Cover, Dynamic World, and WorldCover datasets. Agreement between ground-based and satellite-based classifications was evaluated in a pairwise manner at each point across the 37 point grid, allowing for a basic accuracy assessment of classification consistency. While a full confusion matrix and derived statistical measures such as Cohen's Kappa coefficient would provide a more formal assessment of classification accuracy, the scope of this study and the heterogeneous nature of suburban land cover limited the feasibility of strict pixel-level correspondence across datasets with differing spatial resolutions. As a result, the validation approach in this study is best interpreted as an agreement-based assessment rather than a fully statistical accuracy evaluation, where consistency across multiple independent datasets is used as a proxy indicator of classification reliability.

3. Results

Through the employment of a spread of datasets, programs, and applications, the land cover change in the environment was able to be displayed in both quantitative and qualitative senses, which provided a rich understanding of what occurred to the area of interest, or in this case, Euless, over time. Remote sensing via satellite data helped back the dataset data, which paired well with the field observations with GLOBE Observer. Even though some image chips may not have aligned with the graphical data provided by the satellite information, both types of field work help come together to create a narrative on the types of change that the area of interest has undergone.

When going through the different datasets, there were many agreements on how they interacted with the GLOBE Observer photos that were taken. For instance, the WorldCover 10m dataset showed that the Built-Up (which corresponds to the Built Area of other datasets) for the 900-hectare grid had increased from 2020 to 2021 by almost 50 hectares; however, the tree life had declined by almost 4 hectares, showing a definitive urban development trend. On the actual AOI grid of Euless, the points marked as points 25 and 26 were surrounded by significant vegetation and tree canopy cover. Those points were both residential houses located in what is considered a “green” community in the Hurst-Euless-Bedford region. The Meta/WRI Tree Canopy dataset showed a layer of trees that were highly populous in those areas, which confirmed the satellite data of the other two generalized datasets. Not only were the trees in the region highly prevalent in context to the other points on the 37-point grid, but the trees were also taller, as they were noted to be around 13-14 meters in height. This draws a stark contrast to the majority of the other trees in the region, which average around 5.7 meters in height. While there were a few discrepancies within some smaller subsections of the 100m sampling points when layering 2 or more datasets, such as the Meta/WRI Global Canopy Height and the WorldCover 10m 2020-2021, they followed a highly similar pattern and trend of tree canopy, as there were more trees in some areas than others. If at all, the only inaccuracy with the layers seemed to be the categorization of bare ground, as in points 25 and 26; there seemed to be a discrepancy with how the Global Canopy Height dataset showed that there were trees in the bare ground regions marked by the WorldCover 10m dataset. This seemed to be a pattern as it appeared more than once in the sampling squares. This could very well be explained using the Collect Earth Online software, which allowed for manual categorization of land cover. In the CEO, many areas in the AOI had shadowed areas due to the tree canopy areas, especially around points 25 and 26. Consequently, this allowed for the satellite pictures to not pick up on important surfaces such as bare ground or impervious surfaces like roads, sidewalks, pools, and more. This would help explain those differences in the individual layers in EarthMap since the datasets in the application are derived from the source material of aerial photographs via satellites.

The ESRI dataset seemed to show a significant amount of built-up areas compared to the other datasets, such as the WorldCover 10m 2020/2021. It showed barely any trees, at least visually, so there was a harder time differentiating between what the quantitative data was showing about the trees when there was no color difference showing that there were, in fact, trees present across the entire AOI grid. The bar graphs that were generated in EarthMap showed a majority of built area in 2017 as well as 2024; however, even with the difference in substantial urban development, the trend of fewer trees and vegetation seemed to be present, affirming the notion that Euless has undergone increased levels of urbanization in the past decade, at the very least.

The Landsat Time Series Explorer graphs seemed to be highly reflective of the type of change that was seen by the GLOBE Observer photos that were taken at the beginning of the study. In the past 1 year, there has been increased renovation done on nearby parks and schools, which has yet to be reflected on the graphs, however. The greenery that blanketed nearly all the image chips that were generated in the Landsat Time Series Explorer seemed to have stayed constant through the years. Only when a drastic geographic change, such as the renovations that occurred, did the image chips reflect that. Aside from that, the image chips drew a deep parallel to the actual city on how it was when the photos were taken.

Although, even though there seemed to be little to no change in the landscape, especially in the context of the natural environment, there obviously seemed to be some fluctuation in the NBR as those values were not the same every year, nor did they show a continued constant relationship. In many of the chips, such as point 26, the generated graph showed a slightly linear increase in the NBR over the years from 1985 to 2001, but then changed to a logarithmic plateau from 2001 to 2024. On July 31, 2025, the data point for the NBR drastically increased to 0.509 from 0.476 in 2024, indicating a sudden, significant increase in healthy vegetation in the area. This change would be less surprising considering the context in which point 26 is located in Euless. This could indicate that the areas where there are substantial amounts of tree canopy and forestry amid residential homes have been undergoing a potential urban greening or reforestation initiatives to increase the healthy vegetation and tree canopy despite the trends of urbanization that are noted by all the other datasets, even if they don't show the other aspects of the city as well as their complementary datasets do.

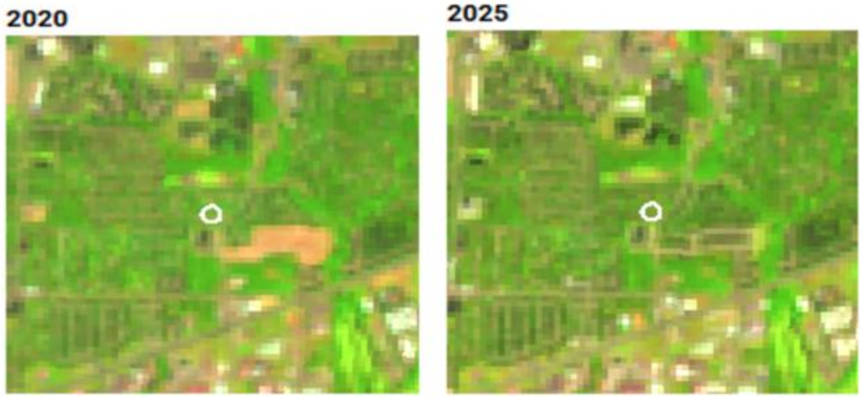

(a) Point 25

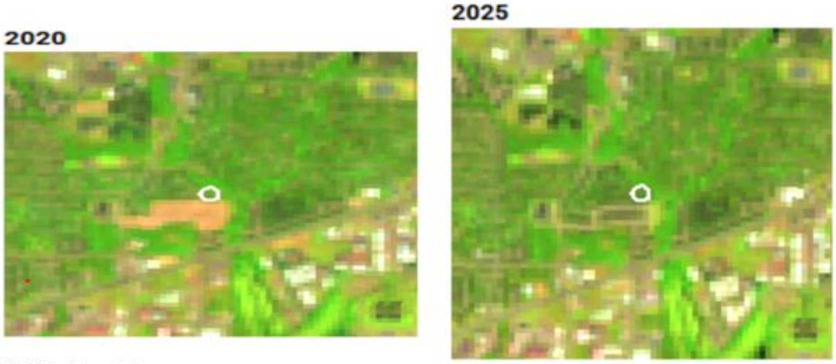

(b) Point 26

Figure 3. Landsat Time Series Explorer visualization showing temporal vegetation dynamics at points 25 and 26 within the AOI. The imagery compares vegetation and canopy conditions across multiple time intervals over a five-year period, highlighting localized stability and variability in vegetation health within residential zones.

This finding complements the ESRI 2017/2024 recording on point 26 specifically, as it showed that the built area in 2017 and 2024 stayed the same. Initially, this may appear counterintuitive, as it would be expected that there should have been an increase in built area considering the pronounced trend of urbanization in Euless. However, it should be noted that the entire southwestern area that includes points 25 and 26 is in residential areas and communities with high levels of tree canopy compared to other areas. This means that there would be no land to urbanize as there is already a planned built settlement there. The only explanation for why that would change would be renovations or a city-wide planning demolition of the community, which would be exceedingly rare.

The number of trees recorded by all of the EarthMap datasets uniformly decreased in all regions. Since all of the datasets that were used in the EarthMap application did not include the present year of 2025, they were unable to show that some areas have begun to increase their healthy vegetation. This could only have been recorded by the Landsat Time Series Explorer program, as it updates more frequently than the EarthMap layers, which it did. Many of the surrounding areas of Euless faced commercialization, where smaller homes or businesses were demolished in favor of larger commercial chains, especially in the fast food industry. This ground observation was highly reflected in every single one of the datasets in EarthMap, as well as the Landsat Time Series Explorer. The utilization of Collect Earth Online with the comparison of the actual GLOBE Observer photographs helped showcase that some residential areas which had more tree canopy had different types of surfacing which was not picked up by some of the datasets; however, in most of the 37 individual smaller 100m sampling squares, the built environment was captured in a detailed manner which could have only been labeled as impervious surfacing in Collect Earth Online with a high confidence rating since it confirmed the findings and visual observations of the GLOBE Observer photos. The study confirms that Euless, Texas, has undergone significant urbanization, characterized by the expansion of built environments. To a high degree, the satellite-backed datasets of EarthMap and Landsat Time Series Explorer seemed to agree with the ground photographs uploaded and analyzed with GLOBE Observer.

4. Discussion

Euless has experienced significant demographic and environmental change over the past decade, reflecting how human settlement patterns interact with land cover over time. While much of the city has seen increased urban development and built-up infrastructure, certain residential areas diverge from this broader trend, particularly in the southwestern portion of the AOI around points 25 and 26. As Euless has become one of the most demographically diverse cities in the Dallas–Fort Worth region, Tongan and Nepalese communities are present in parts of the city, although this study does not directly quantify demographic influence on land cover change. Instead, the observed spatial differences are more reliably interpreted through physical land-use structure, residential continuity, and redevelopment intensity. These neighborhoods exhibit the highest tree canopy coverage and tallest vegetation recorded in the study. WorldCover and Meta/WRI datasets indicate a citywide increase in built-up land between 2020 and 2021, accompanied by an estimated loss of approximately four ha of tree cover; however, points 25 and 26 function as clear anomalies. Tree canopy in these zones remained dense, with average heights of 13–14 meters compared to a citywide average of roughly 5.7 meters, and satellite imagery and GLOBE Observer field photos characterize them as older, established residential neighborhoods with limited redevelopment pressure. Landsat Time Series Explorer data further supports this pattern, as point 26 showed an increase in vegetation health, with NBR values rising from 0.476 in 2024 to 0.509 in 2025.

Together, these findings suggest that long-term residential stability and lower redevelopment turnover may contribute to vegetation persistence within specific neighborhoods. Rather than following a single trajectory of vegetation loss, Euless demonstrates localized variation where social, residential, and land-use factors intersect, producing areas of relative ecological stability amid broader urban expansion. Satellite datasets quantify overall land cover change, while field-based observations provide contextual information on local land-use structure and neighborhood characteristics that help interpret spatial variation within the AOI, or an urbanizing landscape.

Despite these insights, the study could be strengthened by extending both its temporal and spatial scope. Several datasets capture only short-term land cover change, which limits the ability to separate long-term residential stability from temporary fluctuations in vegetation or development. Incorporating longer Landsat or Sentinel time series and higher-resolution canopy data would improve trend reliability, while additional field observations and housing or zoning data could help more directly connect community continuity to redevelopment pressure. These improvements would allow for a clearer understanding of how social structure and land cover interact over time, particularly in neighborhoods that diverge from broader urban patterns.

Despite these findings, several limitations must be acknowledged. One major limitation is the mixed-resolution nature of the datasets used. While high-resolution datasets such as Dynamic World and WorldCover (10 m) capture fine-scale spatial variation, coarser datasets such as Landsat-based products and Meta/WRI canopy height (30 m) generalize land cover features over larger areas. This mismatch can introduce scaling inconsistencies, particularly in suburban environments like Euless where land cover changes occur at very small spatial scales (individual housing lots, narrow tree buffers, and fragmented green space). As a result, some localized vegetation or impervious surface changes may be underrepresented or generalized in coarser datasets.

Additionally, the physical landscape of North Texas presents inherent interpretive complexities. Euless contains a highly fragmented suburban structure with a mix of residential zoning, commercial redevelopment zones, and remaining vegetated pockets. Seasonal variation, drought conditions, and landscaping practices common in Texas suburbs may also affect vegetation indices such as NBR, complicating the distinction between long-term ecological change and short-term environmental variability. Model-based limitations are also present as land cover classification algorithms (such as ESRI and Dynamic World) rely on probabilistic classification, which can introduce uncertainty in transitional zones where built and vegetated classes overlap. Similarly, canopy height models derived from remote sensing may misclassify shadowed regions or underestimate vegetation height in dense residential areas due to occlusion effects.

Despite these limitations, the multi-dataset approach strengthens the reliability of the findings. By integrating high-resolution classification models, long-term Landsat time-series, canopy height estimates, and ground-based validation from GLOBE Observer and Collect Earth Online, the study reduces reliance on any single data source. This cross-validation approach allows for stronger identification of consistent urbanization trends while also revealing localized anomalies that may not appear in individual datasets alone. The combination of multiple spatial resolutions and data types therefore provides both a broad temporal perspective and a fine-scale spatial interpretation of land cover dynamics in Euless.

5. Conclusions

The combined use of remote sensing technologies and field observations provides a comprehensive understanding of how Euless, Texas, has changed over time, both in terms of its physical landscape and its demographic composition, by allowing for the analysis of spatial and temporal patterns in urban development, vegetation health, and tree canopy structure with a level of precision that would not be achievable through ground observations alone. By leveraging multiple datasets, including the WorldCover 10meter dataset, Meta/WRI Tree Canopy and Canopy Height datasets, ESRI layers, Landsat Time Series Explorer graphs, Collect Earth Online classifications, and GLOBE Observer photographs, this study was able to identify and quantify land cover changes across the city while accounting for potential inaccuracies in satellite-derived data, such as misclassified vegetation or shadowed areas in regions with dense tree cover. Overall, the results indicate a clear trend of urban expansion across much of Euless, with built-up areas increasing significantly between 2020 and 2021 and an associated loss of nearly four hectares of tree cover, reflecting broader processes of redevelopment, commercialization, and urban sprawl that are consistent with global patterns of vegetation reduction in growing metropolitan areas, while also highlighting potential implications for local climate, stormwater management, and the maintenance of ecosystem services that are often disrupted by the replacement of natural landscapes with impervious surfaces.

Despite these overall trends, land cover change within Euless is highly heterogeneous, with specific neighborhoods in the southwestern portion of the area of interest, particularly points 25 and 26, demonstrating a markedly different trajectory that is more plausibly associated with differences in neighborhood development history, housing stability, and redevelopment pressure rather than direct demographic or cultural links. These neighborhoods retained dense and healthy tree canopy with vegetation heights of 13 to 14 meters, far exceeding the citywide average of approximately 5.7 meters, while Landsat Time Series Explorer data indicate modest improvements in vegetation health over time, as evidenced by rising NBR values. The preservation of canopy in these areas appears to be associated with long-term residential continuity, larger lot sizes, reduced redevelopment pressure, and the maintenance of established green spaces, indicating that cultural practices and social cohesion may play a critical role in sustaining ecological stability within urban neighborhoods, while also suggesting that demographic settlement patterns can intersect with environmental processes to produce localized resilience even in the context of citywide urbanization.

Ultimately, by comparing neighborhoods experiencing intensive redevelopment with those exhibiting environmental stability, this study highlights the importance of integrating social context into analyses of urban land cover change, demonstrating that the effects of urban growth are not uniform across a single city and that human settlement patterns can significantly influence ecological outcomes, particularly in terms of tree canopy preservation and vegetation health, which are critical for maintaining ecosystem services and quality of life in densely populated areas. The combination of high-resolution satellite data, time-series analysis, and field-based verification provides both quantitative and qualitative insight into these complex interactions, emphasizing the need for urban planning and environmental management strategies that account for the ways in which human communities curate natural landscapes, while also illustrating the broader applicability of remote sensing as a tool for understanding the intertwined dynamics of social structure and cultural practices within urban ecosystems.

Funding: This research was funded by NASA CSR SEES.

Data Availability Statement: Data are available at Zenodo: 10.5281/zenodo.18795944, 10.5281/zenodo.18795671

Acknowledgment: The author would like to acknowledge the support of the 2025 Earth System Explorers (ESE) team, NASA science mentors, and ESE peer mentors. This research was conducted as part of the NASA STEM Enhancement in the Earth Sciences (SEES) high school internship program. The NASA Earth Science Education Collaborative leads Earth Explorers through an award to the Institute for Global Environmental Strategies, Arlington, VA (NASA Award NNX6AE28A). The SEES high school summer intern program is led by the Texas Space Grant Consortium at the University of Texas at Austin (NASA Award NNX16AB89A0).

Conflicts of Interest: The authors declare no conflicts of interest. The funders had no role in the design of the study; in the collection, analyses, or interpretation of data; in the writing of the manuscript; or in the decision to publish the results.

References

Data USA (2023). *Euless, TX.* https://datausa.io/profile/geo/euless-tx.

Jia, J., Sun, H., Jiang, C., Karila, K., Karjalainen, M., Ahokas, E., Khoramshahi, E., Hu, P., Chen, C., Xue, T., Wang, T., Chen, Y., & Hyyppä, J. (2021). Review on active and passive remote sensing techniques for road extraction. *Remote Sensing, 13*(21), 4235. https://doi.org/10.3390/rs13214235.

Kohl, H. (2019) "GLOBE Observer." Globe.gov, NASA, https://observer.globe.gov/.

Kshetri, N. (2023). Remote sensing and satellite imagery. *In Fourth revolution and the bottom four billion: Making technologies work for the poor* (pp. 103–126). University of Michigan Press. https://doi.org/10.3998/mpub.12205632.

Niche (n.d.). *Euless,* TX. Retrieved 8 September 2025, from https://www.niche.com/places-to-live/euless-tarrant-tx/#residents-content.

Singh, K. D. (2000). Role of remote sensing. *In Guidelines on national inventory of village forests* (pp. 25–28). Center for International Forestry Research. http://www.jstor.org/stable/resrep02165.11.

U.S. Census Bureau (2024). American Community Survey 5-year estimates. Retrieved from Census Reporter Profile page for Euless, TX http://censusreporter.org/profiles/16000US4824768-euless-tx/.

Waring, R. H., Way, J., Hunt, E. R., Morrissey, L., Ranson, K. J., Weishampel, J. F., Oren, R., & Franklin, S. E. (1995). Imaging radar for ecosystem studies. *BioScience*, *45*(10), 715–723. https://doi.org/10.2307/1312677.

Weishampel, J. F., Ranson, K. J., & Harding, D. J. (1996). Remote sensing of forest canopies. *Selbyana, 17*(1), 6–14. http://www.jstor.org/stable/41759918.